Impact of the new HNO3-forming channel of the HO2+NO reaction on tropospheric HNO3, NOx, HOx and ozone

Daniel Cariolle, M.J. Evans, M.P. Chipperfield, N. Butkovskaya, Alexandre Kukui, Georges Le Bras

Atmos. Chem. Phys., 8, 4061–4068, 2008
www.atmos-chem-phys.net/8/4061/2008/

Atmospheric Chemistry and Physics

Impact of the new HNO_3-forming channel of the HO_2+NO reaction on tropospheric HNO_3, NO_x, HO_x and ozone

D. Cariolle[1,2], M. J. Evans[3], M. P. Chipperfield[3], N. Butkovskaya[4], A. Kukui[5], and G. Le Bras[4]

[1]Centre Européen de Recherche et Formation Avancée en Calcul Scientifique, Toulouse, France
[2]Météo-France, Toulouse, France
[3]Institute for Climate and Atmospheric Science, School of Earth and Environment, University of Leeds, Leeds, UK
[4]Institut de Combustion, Aérothermique, Réactivité et Environnement, CNRS, Orléans, France
[5]Service d'Aéronomie, IPSL, CNRS, Paris, France

Received: 4 December 2007 – Published in Atmos. Chem. Phys. Discuss.: 11 February 2008
Revised: 24 June 2008 – Accepted: 2 July 2008 – Published: 25 July 2008

Abstract. We have studied the impact of the recently observed reaction $NO+HO_2 \rightarrow HNO_3$ on atmospheric chemistry. A pressure and temperature-dependent parameterisation of this minor channel of the $NO+HO_2 \rightarrow NO_2+OH$ reaction has been included in both a 2-D stratosphere-troposphere model and a 3-D tropospheric chemical transport model (CTM).

Significant effects on the nitrogen species and hydroxyl radical concentrations are found throughout the troposphere, with the largest percentage changes occurring in the tropical upper troposphere (UT). Including the reaction leads to a reduction in NO_x everywhere in the troposphere, with the largest decrease of 25% in the tropical and Southern Hemisphere UT. The tropical UT also has a corresponding large increase in HNO_3 of 25%. OH decreases throughout the troposphere with the largest reduction of over 20% in the tropical UT. The mean global decrease in OH is around 13%, which is very large compared to the impact that typical photochemical revisions have on this modelled quantity. This OH decrease leads to an increase in CH_4 lifetime of 5%. Due to the impact of decreased NO_x on the OH:HO_2 partitioning, modelled HO_2 actually increases in the tropical UT on including the new reaction. The impact on tropospheric ozone is a decrease in the range 5 to 12%, with the largest impact in the tropics and Southern Hemisphere. Comparison with observations shows that in the region of largest changes, i.e. the tropical UT, the inclusion of the new reaction tends to degrade the model agreement. Elsewhere the model comparisons are not able to critically assess the impact of including this reaction. Only small changes are calculated in the minor species distributions in the stratosphere.

1 Introduction

It is well established that the reaction of HO_2 with NO plays a central role in atmospheric chemistry:

$$NO + HO_2 \rightarrow OH + NO_2 \quad \text{(R1)}$$

In the stratosphere, this reaction moderates the effectiveness of the cycle involving HO_x (OH, HO_2) radicals that is an important removal mechanism of ozone (see e.g. Wayne, 2000). In the troposphere Reaction (R1) plays a key role in controlling the interconversion between HO_2 and OH radicals through cycles involving the reactions:

$$OH + CO(+O_2) \rightarrow HO_2 + CO_2 \quad \text{(R2)}$$

$$OH + VOCs(+O_2) \rightarrow HO_2 + \text{products} \quad \text{(R3)}$$

The VOCs include methane, non-methane hydrocarbons and other volatile carbon-containing species. Reaction (R1) is a secondary source of the OH radical (the major tropospheric oxidant), as well as the major source of tropospheric ozone through the conversion of NO to NO_2 followed by NO_2 photolysis. The OH and ozone production rates are limited mainly by the chain termination reaction:

Correspondence to: D. Cariolle
(daniel.cariolle@cerfacs.fr)

Published by Copernicus Publications on behalf of the European Geosciences Union.

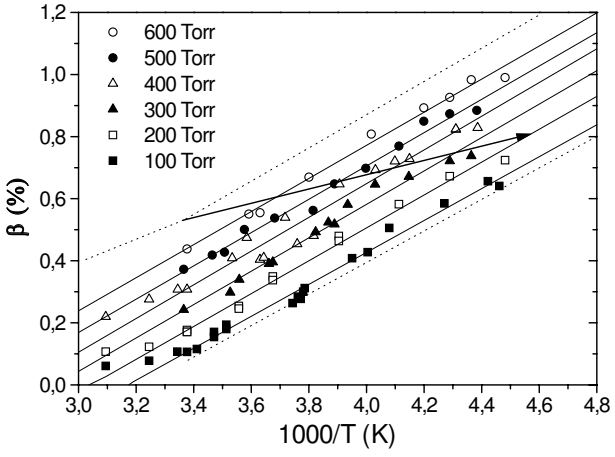

Fig. 1. Pressure and temperature dependences of β=k_{R1b}/k_{R1} in percent. Upper and lower dotted lines represent extrapolation to P=760 and P=50 Torr, respectively. The arrow corresponds to typical β values as a function of altitude from the Earth's surface to the tropopause region.

$$OH + NO_2 + M \rightarrow HNO_3 + M \quad (R4)$$

Another potential significant chain termination reaction is the minor HNO_3-forming channel of the reaction of HO_2 with NO that has been observed in laboratory experiments by Butkovskaya et al. (2005):

$$HO_2 + NO \rightarrow HNO_3 \quad (R1b)$$

The branching ratio, or rate constant ratio, β=k_{R1b}/k_{R1}, for the new Reaction (R1b) was found to range from ~0.2 to 0.8% from 300 K to 200 K, at a pressure of 200 Torr. These first data led to the suggestion that Reaction (R1b) could be a significant loss process of HO_x radicals in the upper troposphere. To assess the potential importance of Reaction (R1b) throughout the troposphere, it appeared necessary to determine the branching ratio β over the full range of tropospheric pressures and temperatures in order to provide a parametrisation of β for atmospheric modelling.

In this paper we first briefly report the experimental measurements of β as a function of pressure and temperature in the ranges 70–600 Torr and 220–320 K. Then, we present 2-D and 3-D model calculations of the impact of Reaction (R1b) on the tropospheric abundances of HNO_3, HO_x, NO_x and ozone by including the parametrisation equation of β obtained from the laboratory experiments. Finally, the model results are compared with observations.

2 Laboratory experiments

The HNO_3-forming channel of the HO_2+NO reaction has been investigated using a turbulent flow reactor (TFR) coupled to a chemical ionisation mass spectrometer (CIMS). The experimental set up has previously been described in detail (Butkovskaya et al., 2005). Briefly, the required high flowrates (60 to 150 SLPM) are obtained by flowing N_2 carrier gas from a liquid nitrogen tank. The working pressure and temperature ranges in the TFR are 70–600 Torr and 220–320 K, respectively. The HO_2 radicals were produced by reaction of H atoms with O_2. The species of interest in the reactive system, HO_2, OH, NO_2 and HNO_3, were detected by CIMS from their reaction with the SF_6^- ion. The branching ratio of Reaction (R1), $\beta = k_{R1b}/k_{R1}$, was obtained by measuring the concentration ratio of the HNO_3 and NO_2 products from channels (R1b) and (R1), respectively.

The calibration procedure of the CIMS signals of HNO_3 and NO_2 is described in detail by Butkovskaya et al. (2007). In order to increase the signal intensity of produced HNO_3, which was a critical factor in reducing experimental uncertainties, the signal was chemically amplified by adding high concentrations of CO and O_2 into the TFR. The chain mechanism (Reactions R1 and R2) that occurred in the TFR is similar to that occurring in chemical amplifiers used to measure peroxy radicals in the atmosphere (e.g. Cantrell and Stedman, 1982). In addition, CO in Reaction (R2) acts as a scavenger of OH produced in Reaction (R1), preventing formation of HNO_3 in the secondary reaction of OH with NO_2 (Reaction R4). The HNO_3 formation in the $OH + NO_2$ reaction contributed up to 10% of the yield from $HO_2 + NO$ reaction at typical concentrations of CO, O_2 and NO used in these experiments, as also calculated by numerical simulation of the kinetics in the reactor (see Butkovskaya et al., 2007 for details).

The branching ratio β was measured at different pressures and temperatures in the ranges 70–600 Torr and 223–323 K. The pressure and temperature dependencies of β are shown in Fig. 1. In the 298–223 K range the temperature dependences for different pressures present a set of nearly parallel straight lines. The linear fit fails at temperatures higher than 298 K, where curvatures were observed for P=100, 200 and 400 Torr. Below 298 K the whole set of data can be described by the simple three-parameter expression of the general form:

$$\beta(P, T) = a/T + bP + c \quad (1)$$

Coefficient a was found by averaging the slopes of the observed temperature dependencies. Coefficients b and c were determined by standard two-parameter least-square fit of the data. The numerical expression of β in percent can be written as:

$$\beta(P, T) = k_{R1b}/k_{R1} = (530 \pm 20)/T\,(\mathrm{K}) + (6.4 \pm 1.3) \times 10^{-4} P\,(\mathrm{Torr}) - (1.73 \pm 0.07) \quad (2)$$

(with 2σ uncertainties). The rate constant k_{R1b} has been derived from this equation by considering the recommended value k_{R1}=$3.5\times10^{-12}\exp(250/T)$ cm^3 molecule^{-1} s^{-1} (Sander et al., 2006). This NASA-JPL evaluation panel

recommended value and the one recommended by the IUPAC panel (Atkinson et al., 2004, updated 2006) are very similar, the IUPAC one being higher by only 14% at 200 K and 10% at 300 K.

3 Model calculations

We have used two atmospheric chemical models to investigate the impact of Reaction (R1b) on atmospheric chemistry. Using the 2-D (latitude-height) stratosphere-troposphere MOBIDIC model (Cariolle and Brard, 1984) it is possible to evaluate the significance of Reaction (R1b) on the global chemical cycles. It is found that this reaction is important in the free troposphere to control the NO_x and HO_x radical contents and the ozone concentration at low latitudes.

We have also used the GEOS-CHEM 3-D tropospheric chemical transport model (e.g. Evans et al., 2005). This model has a more detailed treatment of tropospheric chemical processes and allows an assessment of the impact of Reaction (R1b) under a wider range of conditions and a more critical comparison against tropospheric observations.

3.1 Model simulations and impact on species distributions

The MOBIDIC model has been recently updated to include the Sander at al. (2006) compilation for the reaction rates of atmospheric interest. The dynamical forcing and the numerical scheme for the transport of minor trace species have also been updated (Cariolle and Teyssèdre, 2007).

To investigate the impact of Reaction (R1b) two simulations have been performed. The control simulation (referred to as run **CON2D**) does not include Reaction (R1b) while simulation **NEW2D** includes Reaction (R1b) with $k_{R1b}=\beta\times k_{R1}$ and β given by Eq. (2). Each simulation was integrated over 8 years. The model outputs are compared for the last simulated year when steady-state is reached.

The GEOS-CHEM 3-D tropospheric CTM has been used for a number of studies focused on tropospheric O_3-OH-NO_x budgets (e.g. Bey et al., 2001; Evans and Jacob, 2005 and references therein). The GEOS-CHEM model is driven by assimilated winds calculated by the Goddard Earth Observing System at $4^\circ\times5^\circ$ horizontal resolution and 30 levels in the vertical. Surface sources of NO_x are 42 Tg N yr^{-1} (anthropogenic, biomass burning and soil) while upper troposphere sources amount to 4 Tg N y^{-1} (lightning and aircraft). The model description is given by Bey et al. (2001).

In this study we have used the same model version as Evans and Jacob (2005) who investigated the impact of new laboratory studies on the aerosol hydrolysis of N_2O_5. In that study Evans and Jacob found that the newer slower rate of conversion of N_2O_5 to HNO_3 on aerosols increased the average tropospheric budgets of NO_x (by 7%), O_3 (4%), and OH (8%), bringing the model into better agreement with observations. Here we repeat the approach of Evans and Jacob (2005) and include Reaction (R1b).

The 3-D model was run for 2 simulations of 2 years each. The control run (**CON3D**) was similar to a run from Evans and Jacob (2005) using the aerosol parameters from their Table 1. Run **NEW3D** was the same as run **CON3D** but included Reaction (R1b) in the same way as for the MOBIDIC model. The first year of the model run was treated as a spin up and results from the second year were used for analysis.

3.1.1 Impact on nitrogen species

Figure 2a shows the rate of HNO_3 formation by Reaction (R1b) and by Reaction (R4) between NO_2 and OH at the equator in March using output from run **NEW2D**. It appears that Reaction (R1b) becomes a significant channel for HNO_3 formation between 7 to 16 km in the cold upper troposphere region. The ratio Ra between the rates of HNO_3 formation by these 2 reactions is equal to: $Ra=([NO].[HO_2]/[NO_2].[OH]).(k_{R1b}/k_{R4})$. The first term of the product corresponds to an "atmospheric" component that depends on the NO_x and HO_x profile concentrations. This term increases from a value of 40 at ground level to a peak value of about 220 at 10 km. The second term k_{R1b}/k_{R4} shows an increase from 0.004 at ground level to 0.01 at 15 km. The differences in the altitude profiles of NO_x and HO_x appears as important as the temperature dependency of the Reaction (R1b) to determine its effectiveness. Both terms act in the same direction, so the HNO_3 concentration increases from ground to the UT when Reaction (R1b) is introduced in the 2-D model.

Figure 3 shows the variations in the HNO_3 concentration between 2-D model runs **NEW2D** and **CON2D** for the month of March. The relative effect is largest at the cold equatorial tropopause with an increase over 30%. HNO_3 increases by about 10% in the lower stratosphere and by up to more than 100% in the upper stratosphere. However, the HNO_3 concentrations are quite small compared to those of the other NO_y species, so we expect little impact of Reaction (R1b) at those altitudes.

The increase in the HNO_3 concentration by Reaction (R1b) changes the ratio between NO_x and HNO_3. Model results show that the concentrations of NO_x decreases by 20 to 30% in the troposphere. In particular Fig. 3 shows that the NO concentration decreases by more than 30% at low latitudes in the middle-upper troposphere.

Equally, Fig. 4 shows the zonal mean differences between runs **CON3D** and **NEW3D** for selected species in March. In run **NEW3D** NO_x decreases everywhere ranging from -5% in the Northern Hemisphere (NH) mid-latitudes to -35% in the tropical and Southern Hemisphere (SH) upper troposphere (UT). The 3-D model shows more latitudinal variation in the modelled NO_x response than the 2-D model. In the 3-D model, near the surface, the smallest relative NO_x decrease occurs in the northern mid-latitudes in regions of high NO_x

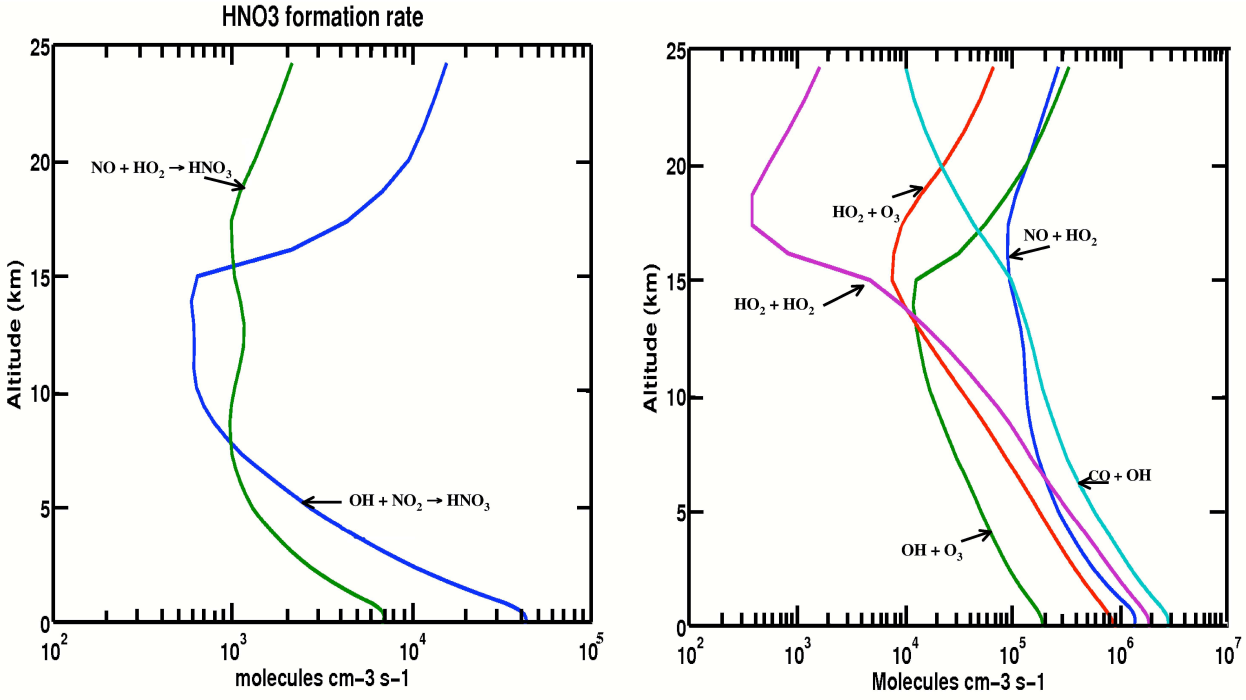

Fig. 2. Left panel **(a)**: rate of formation of HNO_3 at the equator for March calculated from the 2-D model run **NEW2D** for the reactions OH+NO_2 (blue line) and NO+HO_2 (green line). Right panel **(b)**: rate of the main reactions that control the conversion between OH and HO_2 at the equator calculated from the 2-D model for the same month.

close to emissions sources. In the Southern Hemisphere, away from fresh pollution, the long transport timescales for NO_x allow a larger impact of Reaction (R1b). The 2-D model, with its simpler treatment of the troposphere, misses this effect partly because of specification of fixed surface mixing ratios in the 2 runs. Except very near the surface, HNO_3 increases everywhere in the 3-D model and by up to 35% in the tropical UT. Overall, the MOBIDIC and GEOS-CHEM models exhibit similar responses to the introduction of reaction (R1b).

3.1.2 Impact on HO_x species

These perturbations in the nitrogen species budget impact the distribution of HO_x. Figure 2b shows the rates of the main reactions that control the OH:HO_2 ratio. As can be seen, Reaction (R1) is a major player controlling this ratio in the middle troposphere – lower stratosphere at the equator (5–20 km). Consequently, the tropospheric NO decrease due to Reaction (R1b) tends to slow down the conversion of HO_2 to OH by Reaction (R1).

The global tropospheric OH budget is difficult to establish. It results from a delicate balance between production processes dominated by water vapour, methane and acetone (e.g. Arnold et al., 2004) decompositions and destruction by reactions involving HO_x radicals that form back water vapour. As discussed by Butkovskaya et al. (2005) an additional effect of Reaction (R1b) is to decrease the HO_x concentrations. Larger HNO_3 concentrations are formed that are subsequently washed out, thus removing a larger part of the HO_x radicals. In addition, the HO_x removal by the reaction between OH and HNO_3 can also be enhanced.

The net effect in the MOBIDIC model simulations is a decrease of the OH concentration by about 10 to 20% in the middle and upper troposphere for latitudes lower than 40° (Fig. 3), and a smaller increase of the HO_2 concentration by 10% in the upper troposphere at the same latitudes between 10 to 15 km.

The GEOS-CHEM model shows a response consistent with the MOBIDIC model with however a larger contrast between the two hemispheres. The OH concentration decreases by −6% at the surface at NH mid-latitudes, by −15% at SH mid-latitudes, but as much as −20% in the tropical UT. However, the decrease in NO_x modifies the OH:HO_2 ratio and tends to increase the HO_2 concentration in some locations, e.g. the tropical UT, even though the overall net HO_x production is reduced.

In run **CON3D** the mass-weighted global annual mean tropospheric OH is $1.12\times10^6\,cm^{-3}$ and becomes $0.97\times10^6\,cm^{-3}$ in run **NEW3D**, a decrease of 13%. This is a very large relative change as modelled mean OH is a quantity that is typically well buffered against changes as revisions to model HO_x photochemistry are implemented. However, this large relative change still leaves the model

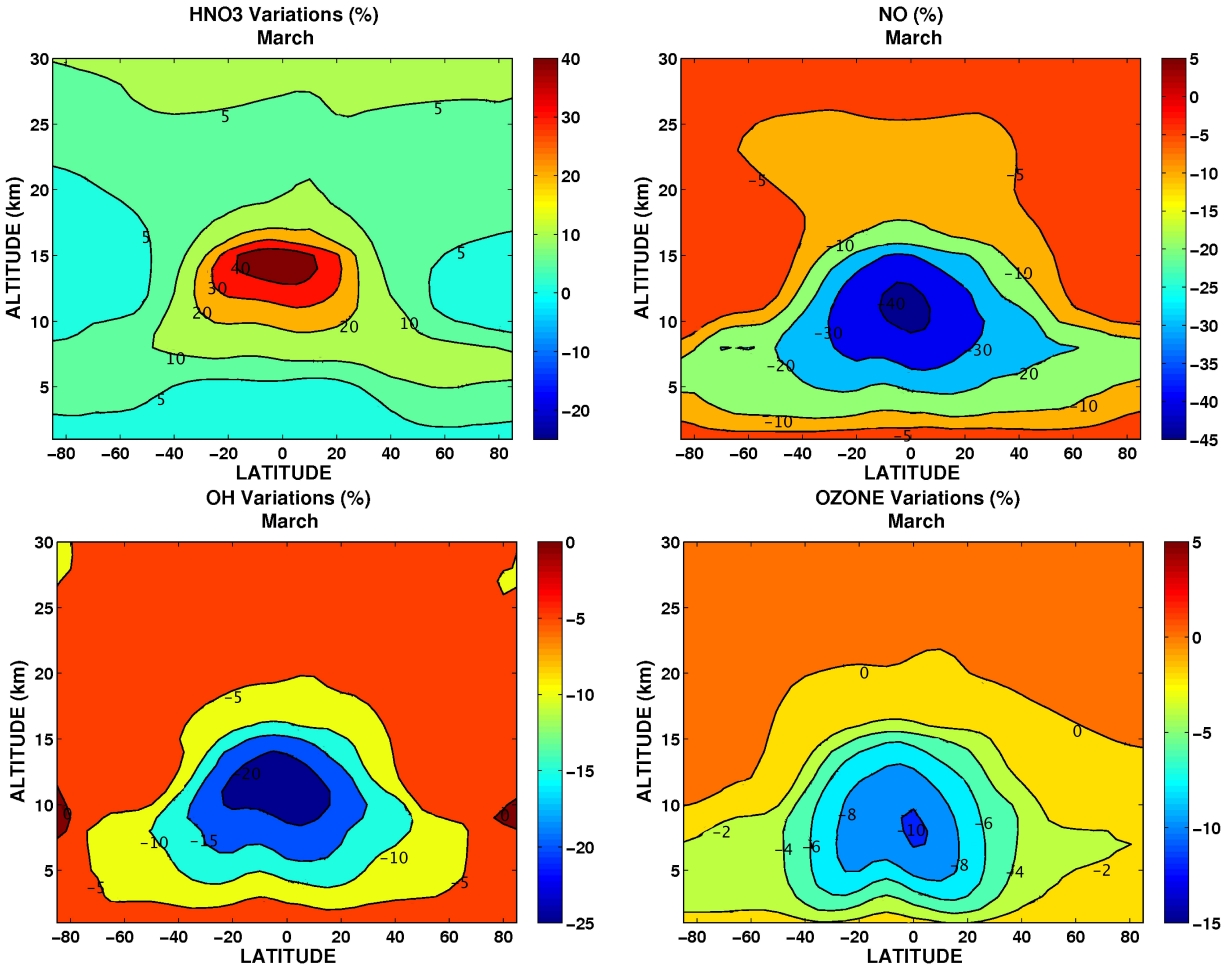

Fig. 3. Differences (%) in the concentration of HNO_3 (upper left), NO (upper right), OH (lower left) and O_3 (lower right) between 2-D model runs **NEW2D** and **CON2D** for the month of March. Negative contours indicate smaller values in run **NEW2D**.

within the range of mean OH values derived from methylchloroform observations: $1.07{+}0.09/{-}0.17{\times}10^6$ (Krol et al., 1998), $1.16{\pm}0.17{\times}10^6$ (Spivakovsky et al., 2000) and $0.94{\pm}0.13{\times}10^6\,cm^{-3}$ (Prinn et al., 2001). Those figures are consistent with recent evaluations by Bloss et al. (2005) that give a mean northern and southern hemispheric OH concentrations of $0.91\times10^6\,cm^{-3}$ and $1.03\times10^6\,cm^{-3}$ respectively, evaluations in very good agreement with the mean value in **NEW3D**.

The OH decrease will slow the destruction rates of important long-lived species which are sources of radicals or have large global warming potentials. For instance, CH_4 contributes significantly to the atmospheric greenhouse forcing. The major sink of CH_4 is its reaction with OH:

$$CH_4 + OH \rightarrow CH_3 + H_2O \qquad (R5)$$

The CH_4 chemical lifetime, τ_{CH_4}, can therefore be evaluated by dividing its total atmospheric content by the integration over the whole domain of its destruction rate:

$$\tau_{CH_4} = \frac{\int [CH_4].dv}{\int k_{OH+CH_4}[OH][CH_4].dv}$$

Evaluations of τ_{CH_4} from the MOBIDIC outputs give a lifetime of 9.6 years for run **CON2D** and 10.1 years for run **NEW2D**. Thus, the CH_4 lifetime is increased by about 5% when Reaction (R1b) is introduced in the model.

3.1.3 Impact on tropospheric ozone

These perturbations in the HO_x and NO_x distributions have an impact on the tropospheric O_3 budget. Ozone production via the cycles involving Reactions (R2) and (R3) is reduced due to the NO and OH decreases. The decrease calculated by MOBIDIC is largest at low latitudes between 5 and 10 km (Fig. 3), with a maximum of about -10%. This response is

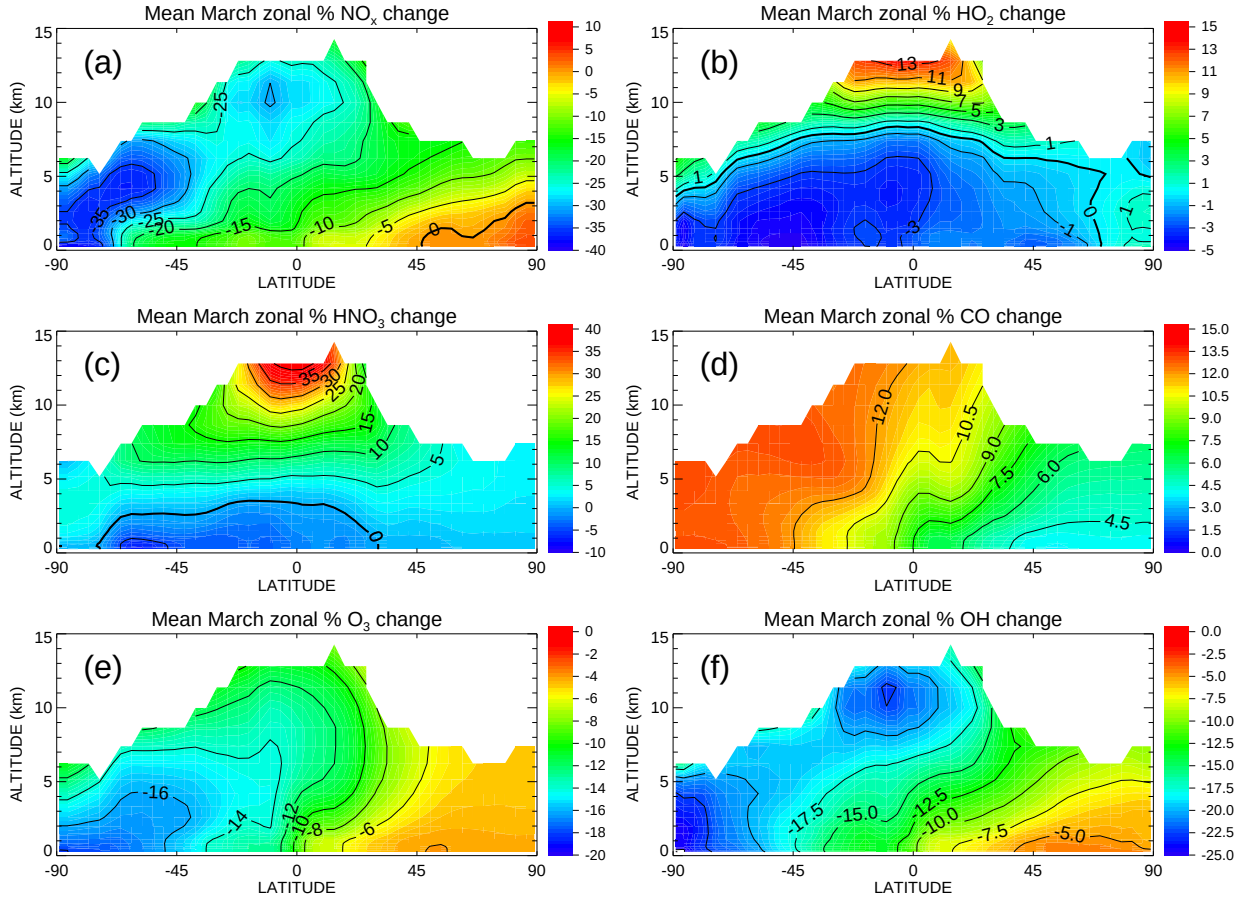

Fig. 4. Mean differences (%) for the month of March between 3-D model runs **NEW3D** and **CON3D** for **(a)** NO_x, **(b)** HO_2, **(c)** HNO_3, **(d)** CO, **(e)** O_3 and **(f)** OH. Negative contours indicate smaller values in run **NEW3D**.

not very sensitive to the season. The GEOS-CHEM model gives a similar response in the UT, but produces a larger O_3 decrease in the SH lower troposphere. This is due to the larger NO_x decrease that is found in this hemisphere away from major surface sources. The decrease in NO_x has the impact of decreasing O_3 throughout the troposphere ranging from −6% to −16%.

3.2 Comparison with observations

Figure 5 compares modelled profiles of NO_x and HNO_3 from runs **CON3D** and **NEW3D** with a compilation of aircraft observations mapped onto a monthly $4° \times 5°$ grid (Emmons et al., 2000). For this comparison the appropriate grid box of the model was sampled and then the results averaged over all the observation points. As discussed above, the NO_x concentrations in run **NEW3D** are lower than run **CON3D**, while HNO_3 is generally larger. The region where the modelled change is most significant is in the tropical UT where **NEW3D** agrees less well with the observations, especially for NO_x. Elsewhere the modelled changes are not large compared with the model-observation differences.

Figure 6 compares annual mean modelled ozone profiles with the climatology of Logan (1999). In the middle troposphere both model runs agree fairly well with the observations, although run **CON3D** is, on average, closer. The model underestimate of observations of O_3 in the 7–10 km range reflects issues with an overestimate in the GEOS tropopause mass flux which is in excess. To maintain a 500 Tg yr^{-1} cross tropopause O_3 flux, lower than observed O_3 concentrations are necessary within the model stratosphere. The mean ratio between model and observed in run **CON3D** is 1.0078 while in run **NEW3D** it is 0.9148. The total tropospheric O_3 in run **CON3D** is 284 Tg while in run **NEW3D** it is 259 Tg. There are no direct observations of this total but these values are at the lower range of modelled values (see Stevenson et al., 2006).

4 Conclusions

The minor HNO_3-forming channel of the reaction between NO and HO_2 has a significant impact on tropospheric chemistry. It leads to a reduction of NO_x and OH radical

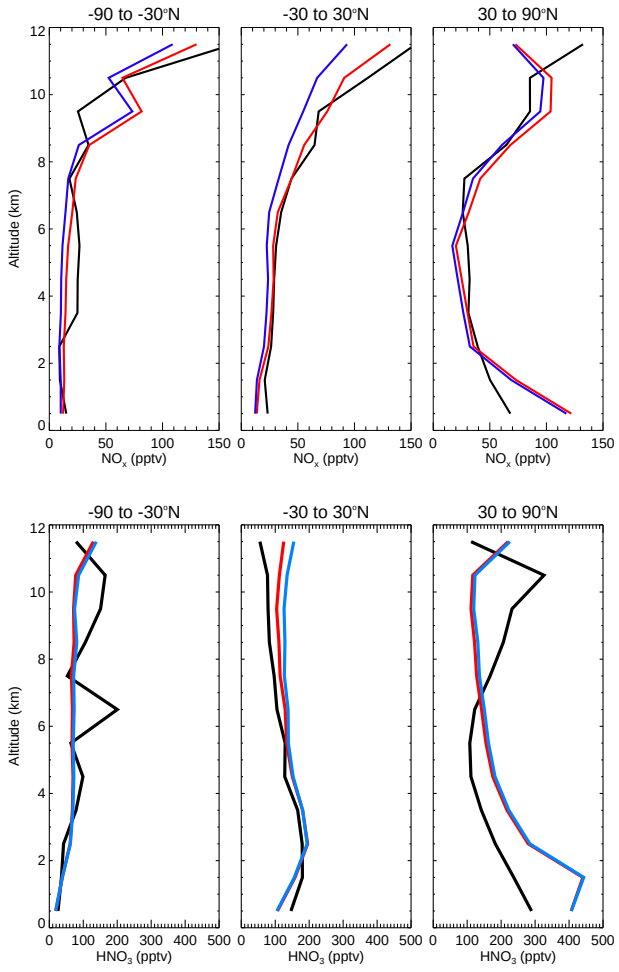

Fig. 5. Comparison of profiles (pptv) of NO_x (top) and HNO_3 (bottom) averaged over 3 latitude bands (left 90° S–30° S, centre 30° S–30° N, right 30° N–90° N) from 3-D model run **CON3D** (red line), run **NEW3D** (blue line) and observations (Emmons et al. (2000), black line).

concentrations that produces an ozone increase in the troposphere. Due to the temperature dependence of the reaction, the effects on the species distributions are generally largest at the equatorial mid and upper troposphere where the temperatures are low, and at high latitudes in the SH. In those regions the O_3 concentration decreases by about 10% when Reaction (R1b) is taken into account.

The OH reduction induced by Reaction (R1b) can also increase the lifetime of the long-lived species whose destruction proceeds mainly by reaction with this radical. This is the case for CH_4 whose lifetime reaches 10.1 years against 9.6 years when Reaction (R1b) is neglected.

Reaction (R1b) has been established by laboratory measurements and should therefore be included in photochemical models. Comparison of our 3-D model with observations of NO_x, HNO_3 and O_3 suggests that the overall agreement

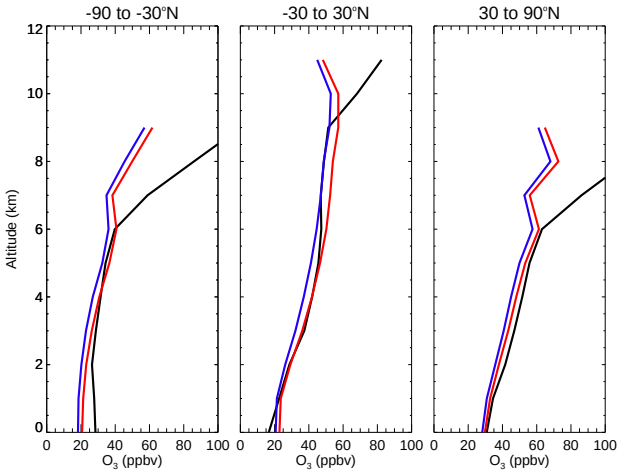

Fig. 6. As Fig. 5 but for O_3 (ppbv) compared with observed climatology of Logan (1999).

tends to worsen when the reaction is included. This, therefore, points to other outstanding uncertainties in tropospheric NO_x:HNO_3 partitioning. Possible causes of these differences need further investigation in the laboratory and with models.

The present evaluation has been performed at global scale with a representation of the atmospheric chemistry adequate mostly for the free troposphere. It is expected that the impact of Reaction (R1b) could be different for specific regions where background species concentrations can vary from the mean values produced by the large-scale models. This, for instance, could be the case in boundary layers over continents or polluted areas. Thus, the present study should be complemented by air quality model simulations to obtain a more comprehensive picture of the possible regional and local influences of Reaction (R1b) on the atmospheric chemistry.

Acknowledgements. This work was supported by the European Union FP6 Integrated Projects SCOUT-O3 (http://www.ozone-sec.ch.cam.ac.uk) and QUANTIFY (http://www.pa.op.dlr.de/quantify/), and the french LEFE/CHAT INSU programme (http://www.insu.cnrs.fr).

Edited by: A. Hofzumahaus

References

Arnold, S. R., Chipperfield, M. P., Blitz, M. A., Heard, D. E., and Pilling, M. J.: Photodissociation of acetone: Atmospheric implications of temperature-dependent quantum yields, Gephys. Res. Lett., 31, L07110, doi:10.1029/2003GL019099, 2004.

Atkinson, R., Blauch, D. L., Cox, R. A., Crowley, J., Hampson Jr., R. F., Hynes, R. G., Jenkin, M. E., Rossi, M. J., and Troe, J.: Evaluated kinetic and photochemical data for atmospheric chemistry: Volume I – gas phase reactions of O_x, HO_x, NO_x and SO_x

species, Atmos. Chem. Phys., 4, 1461–1738, 2004, Updated at http://www.iupac-kinetic.ch.cam.ac.uk, 2006.

Bey, I., Jacob, D. J., Yantosca, R. M., Logan, J. A., Field, B. D., Fiore, A. M., Li, Q., Liu, H. Y., Mickley, L. J., and Schultz, M. G.: Global modelling of tropospheric chemistry with assimilated meteorology: Model description and evaluation, J. Geophys. Res., 106, 23 073–23 096, 2001.

Bloss, W., M. J. Evans, J. D. Lee, R. Sommariva, D. E. Heard and M. J. Pilling: The oxidative capacity of the troposphere: Coupling of field measurements of OH and a global chemistry transport model, Faraday Discuss., 130, 425, doi:10.1039/b419090d, 2005.

Butkovskaya, N. I., Kukui, A., Pouvesle, N., and Le Bras, G.: Formation of nitric acid in the gas-phase HO_2+ NO reaction: Effects of temperature and water vapor, J. Phys. Chem. A, 109, 6509–6520, 2005.

Butkovskaya, N. I., Kukui, A., and Le Bras, G.: HNO_3 forming channel of the HO_2+NO reaction as a function of pressure and temperature in the ranges of 72–600 Torr and 223–323 K, J. Phys. Chem. A, 111, 9047–9053, 2007.

Cantrell, C. A. and Stedman, D. H.: A possible technique for the measurement of atmospheric peroxy radicals, Geophys. Res. Lett., 9, 846–849, 1982.

Cariolle, D. and Brard, B.: The distribution of ozone and active stratospheric species: Result of a two-dimensional atmospheric model, in: Atmospheric Ozone, edited by: Zerefos, C. S. and Ghazi, A., D. Reidel, Higham, Mass., 77–81, 1984.

Cariolle, D. and Teyssèdre, H.: A revised linear ozone photochemistry parameterization for use in transport and general circulation models: Multi-annual simulations, Atmos. Chem. Phys., 7, 2183–2196, 2007, http://www.atmos-chem-phys.net/7/2183/2007/.

Emmons, L. K., Hauglustaine, D. A., Muller, J.-F., Carroll, M. A., Brasseur, G. P., Brunner, D., Staehelin, J., Thouret, V., and Marenco, A.: Data composites of airborne observations of tropospheric ozone and its precursors, J. Geophys. Res., 105, 20 497-20 538, 2000.

Evans, M. J. and Jacob, D. J.: Impact of new laboratory studies of N_2O_5 hydrolysis on global model budgets of tropospheric nitrogen oxides, ozone, and OH, Geophys. Res. Lett., 32, 1–4, 2005.

Krol, M., Leeuwen, P. J., and Lelieveld, J.: Global OH trends inferred from methyl-chloroform measurements, J. Geophys. Res., 103, 10 697–10 711, 1998.

Logan, J. A.: An analysis of ozonesonde data for the troposphere: Recommendations for testing 3-D models and development of a gridded climatology for tropospheric ozone, J. Geophys. Res., 104, 16 115–16 149, 1999.

Prinn, R. G., Huang, J., Weiss, R. F., et al.: Evidence for substantial variations in atmospheric hydroxyl radicals in the past two decades, Science, 292, 1882–1888, 2001.

Sander, S. P. , Friedl, R. R., Golden, D. M., Kurylo, M. J., Moortgat, G. K., Keller-Rudek, H., Wine, P. H., Ravishankara, A. R., Kolb, C. E., Molina, M. J., Finlayson-Pitts, B. J., Huie, R. E., and Orkin, V. L.: Chemical Kinetics and Photochemical Data for Use in Atmospheric Studies, JPL Publication 06-2, Evaluation no. 15, 2006.

Spivakovsky, C. M., Logan, J. A., Montzka, S. A., et al.: Three-dimensional climatological distribution of tropospheric OH: Update and evaluation, J. Geophys. Res., 105(D7), 8931–8980, 2000.

Stevenson, D. S., Dentener, F. J., Schultz, M. G., et al.: Multimodel ensemble simulations of present-day and near future tropospheric ozone, J. Geophys. Res., 111, D08301, doi:10.1029/2005JD006338, 2006.

Wayne, R.: Chemistry of Atmospheres, Oxford University Press, 2000.